Aldehyde and formic-acid hydration bonding dynamics: hydrogen bond and surface stress transition

Jiasheng Chen[1,2], Chuang Yao[2,*], Xi Zhang[3], Chang Q Sun[4,*], Yongli Huang[1,*]

Abstract

Solvation of aldehydes and formic acids has an important impact to health care because these additives can damage DNA and denature proteins causing cancers with the mechanism behind remaining great challenge. From the perspective of solvent hydrogen bond (O:H-O or HB with ":" being the electron lone pair of oxygen) transition from the mode of the ordinary water to the hydrating states, we examined the solvation bonding dynamics and the solute capabilities of O:H-O bond and surface stress transition using differential Raman spectroscopy and contact angle detection. Results suggest that besides the short-range O:H van der Waals (vdW) bond, the H↔H and O:⇔:O repulsive intermolecular interactions, and the molecular dipolar polarization play important roles in disrupting the solution network and surface stress. Observations may infer the manner of DNA fragmentation by aldehyde and formic acid disruption.

[1] School of Materials Science and Engineering, Xiangtan University, Xiangtan 411105 (1403277520@qq.com; huangyongli@xtu.edu.cn)

[2] Chongqing Key Laboratory of Extraordinary Bond Engineering and Advanced Materials Technology (EBEAM), Yangtze Normal University, Chongqing 408100, China (yaochuang@yznu.cn)

[3] Institute of Nanosurface Science and Engineering, Shenzhen University, Shenzhen 518060, China; (Zh0005xi@szu.edu.cn)

[4] NOVITAS, School of EEE, Nanyang Technological University, Singapore 639798 (ecqsun@gmail.com)

1. Introduction

Aldehydes are the most common indoor pollutants that are harmful to our health. Characterized by a wide range of sources, high level, toxicity, and long duration, aldehydes have been recognized as key factors of cancer development. As an indoor pollutant, aldehyde contamination cause damage of the DNA-protein cross-linking and binding to form adducts [1, 2]. Formaldehyde and acetaldehyde adsorption damages the DNA of human peripheral blood lymphocytes [3, 4]. Likewise, formic acids play an important role in biomedical and cosmetic applications [5]. Oral administration of concentrated acetic acid can corrode the mouth and cause oral mucosa, esophageal and gastric mucosal damage, and even lead to gastric perforation [6]. Once the acetic acid is absorbed by human body, hemolysis, acute renal failure, acute liver failure, disseminated intravascular coagulation and circulatory shock may occur [7, 8]. There are numerous applications of propionic acid in the food and chemical industries, such as a food preservative and as a component in plasticizers, perfumes and pharmaceuticals e. Current research is mainly focused on the possible mechanism of DNA breakage and binding. Molecular scale understanding of DNA-aldehyde and aldehyde-aldehyde interactions and the functionalities of formic acids remains a challenge.

From the perspective of solvent hydrogen bond transition from the mode of the ordinary water to the hydrating states and the solution surface stress, we examined the solvation dynamics and the solute capabilities of aldehydes and formic acids using differential Raman spectroscopy and contact angle detection. Results suggest that beside the short-range O:H vdW bond, H↔H and O:⇔:O repulsive interactions, molecular dipolar interaction plays an important role in disrupting the solution network and surface stress.

2. Principles

2.1. Hydrogen bond (O:H-O) cooperativity

Solvation of organic crystal dissolves the crystal into individual molecular dipoles surrounded with protons H^+ or electron lone pairs ":" pertained to O anions. The molecular H^+ and ":" interact with their alike or unlike of the solvent H_2O to form the O:H vdW bond, H↔H anti-HB or O:⇔:O super-HB repulsive interactions, as they do in solutions of acid, base, and salt [11-13]. An addition of excessive H^+ or electron lone pair ":" will form the inter-proton and inter-lone-pair interaction, which called the H↔H anti-HB or Oe:e:O super-HB, accordingly. The O:H-O bonds in the hydration shells, or solute –solvent interface, relax cooperatively, which govern the performance of the solution such as

the surface stress, solution temperature, and the critical pressures and temperatures for phase transition [13].

Therefore, one needs to understand the O:H-O bonds transition from the vibration mode of ordinary water to the hydrating states in terms of their stiffness (frequency shift) and number fraction (phonon abundance). The O:H-O bond consists the weaker O:H intermolecular (in terms of bond energy and vibration frequency: ~0.1 eV; ~200 cm^{-1}) and the stronger H-O intramolecular (~4.0 eV; 3200 cm^{-1}) short-range interactions. The Coulomb repulsion between electron pairs on adjacent oxygen ions couples the O:H-O bond and ensures its cooperative relaxation in segmental length and vibration frequency [14] as summarized in Table 1. As a consequence of O:H-O bond relaxation and electron polarization or depolarization, the solution surface stress varies with solute concentration and external excitation compared with the standard situation of water at 277 K [15, 16].

Table 1. O:H-O segmental cooperative relaxation in length, vibration frequency, and surface stress with respect to d_{L0} = 1.6946 Å, d_{H0} = 1.0004 Å, ω_{H0} = 3200 cm^{-1}, ω_{L0} = 200 cm^{-1}, γ_s = 72.5 mN/m at 277 K upon excitation by heating, compression, molecular undercoordination (skin, cluster, droplet, nanobubble) and acid, base, salt, alcohol solvation [15, 16].*

		Δd_H	$\Delta\omega_H$	Δd_L	$\Delta\omega_L$	$\Delta\gamma_s$	Remark	Ref
liquid water	heating	<0	>0	>0	<0	<0	d_L elongation; d_H contraction; fluctuation	[17]
	under-coordination					>0	d_H contraction; d_L elongation; polarization; supersolidity	[18]
	compression	>0	<0	<0	>0	-	d_L compression; d_H elongation	[13]
aqueous solution	YX salt	<0	>0	>0	<0	>0	Y^+ and X^- polarization	[19-21]
	HX acidic					<0	H↔H fragilization; X^- polarization	[11]
	YOH basic	>0 <0	>0 <0	>0 <0	>0 <0	>0	O:⇔:O compression; Y^+ polarization; solute H-O contraction	[12]
	alcohol	>0	<0	>0	<0	-	intermolecular interaction; solute dipolar induction	[22]

*X = F, Cl, Br, I; Y = Li, Na, K, Rb, Cs.

As a strongly correlated and fluctuating system, water prefers the statistic mean of the tetrahedrally-coordinated, two-phase structure in a bulk-skin or a core-shell manner of the same geometry but

different O:H-O bond lengths. The O:H vdW bond and the H-O bond segmental disparity and the O-O coupling allow the segmented O:H-O bond to relax oppositely – an external stimulus dislocates both O ions in the same direction but by different amounts. The softer O:H vdW bond always relaxes more than the stiffer H-O bond with respect to the H^+ coordination origin. The ∠O:H-O containing angle θ relaxation contributes only to the geometry and mass density. The O:H-O bond bending has its specific vibration mode that does not interfere the H-O and the O:H stretching vibrations [20].

2.2. Differential Phonon Spectrometrics (DPS)

The Raman spectroscopy provides a powerful tool monitoring the O:H-O bonding dynamics with high precision. A Raman spectral peak features the Fourier transformation of all bonds vibrating in the same frequency from the real space, irrespective of their locations or orientations in the liquid, solid, or vapor phase of the same substance. One can only probe the statistic mean of the vibrations and its fluctuation excited by external stimuli. The spectral peak frequencies correspond to the respective bond stiffness and the peak area to the abundance that is proportional to the number of bonds contributed [15]. The frequency shift $\Delta\omega_x$ represents, in the first order approximation, the stiffness of the O:H vdW bond stretching vibration and H-O cooperative relaxation as a function of the segmental length d_x and energy E_x [23],

$$\Delta\omega_x \propto \sqrt{E_x/\mu_x}\,/\,d_x \propto \sqrt{(k_x + k_c)/\mu_x} \tag{1}$$

The subscript x = L denotes the O:H vdW characterized by the stretching vibration frequency at ~200 cm^{-1} and x = H denotes the H-O bond with characteristic phonon frequency of ~3200 cm^{-1} in the bulk water. The k_x and k_C are the force constants or the second differentials of the intra/inter molecular interaction and O-O Coulomb coupling potentials. The k_C is the coupling by O-O repulsion. The $\Delta\omega_x$ also varies with the reduced mass μ_x of the specific x oscillator. However, from the O:H-O bond Raman spectra, one could hardly be able to gain quantitative information on the transition of the stiffness, fraction, and fluctuation order of bonds by solvation.

Compared with the convention of Gaussian decomposition, the differential phonon spectrometrology (DPS)[24, 25] merely purifies the transition of the phonon stiffness (frequency shift), abundance (peak area), and fluctuation order (linewidth) by differencing the spectra collected from water before and after solvation upon all spectra peak areas being normalized. To gain quantitative information on the

number fraction of O:H-O bonds transiting from water to the hydration shells, one can integrate phonon abundance gain or the DPS peak area, called the fraction coefficient for the specific x peak as a function of solute concentration C,

$$f_x(C) = \int_{\omega_m}^{\omega_M} \left[\frac{I_{solution}(C,\omega)}{\int_{\omega_m}^{\omega_M} I_{solution}(C,\omega)d\omega} - \frac{I_{H_2O}(0,\omega)}{\int_{\omega_m}^{\omega_M} I_{H_2O}(0,\omega)d\omega} \right] d\omega . \quad (2)$$

The spectral subtraction upon the peak area normalization minimizes the "artefacts" of detection such as the mode reflectivity. The "artefacts" may contribute to the intensity and the shape of a peak but negligible to the transition of the phonon stiffness and phonon abundance from the ordinary water reference to the solvated states [26].

Figure 1a illustrates the H-O phonon DPS for the skins of water and ice. The DPS distils the phonon abundance only in the skins as a component presenting above the x-axis, which equals the abundance loss of the ordinary HBs as a valley below the axis. This process removes the common spectral features shared by the intermediate transition from the bulk to the skin. Inset a shows the raw Raman ω_H spectroscopy of water (in blue, at 25°C) and ice (red, at -20 and -15°C) [28] collected at 87° (peaks toward higher frequency) and 0° with respect to the surface normal and water. This DPS strategy allows us to discriminate the behavior of the skin O:H-O bonds from those of the bulk water and ice. The skins of water and ice share the same ω_H of 3450 cm^{-1}. The peak intensity changes with the scattering conditions of fice and water [29].

For aqueous solvation, the removed area is the mixture of the ordinary eater and the high-order hydration shells, which is out of concern as one needs only to focus on the bond transformation within the closest hydration shells. A hydration shell may have one, two or more subshells, depending on the nature and size of the solute. The size and charge quantity determine its local electric field intensity that is subject to the screening by the local H_2O dipoles and modified by the solute-solute interactions.

As ""artefacts"" of phonon spectroscopy, the cross-section of mode reflectivity contribute to the peak shape and the spectral intensity. However, experimental "artefacts" never contribute to the transition of phonon abundance and stiffness upon solvation. As Figure 1b illustrated, the spectral intensity varies significantly with the type of the aldehyde solutes at the same concentration due to the demonstrated

mode reflectivity. The DPS of the aldehyde solvation resolve hardly the spectral difference. One can thus minimize such "artefacts" in the DPS detection by normalizing the specific peak area. Furthermore, the relative reflectivity changes in the 10^{-3} order when the NaCl solution is heated from 0 and 300º C under high pressure, which is within the tolerance of most available means [27].

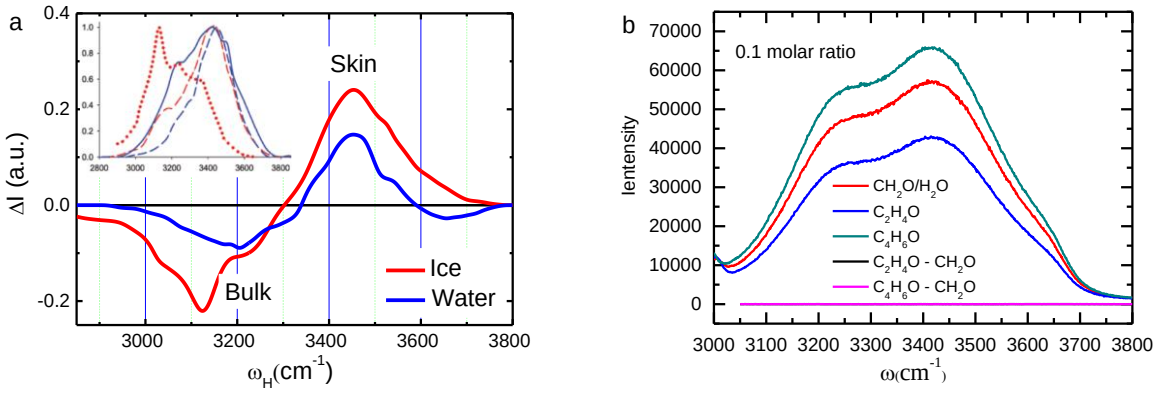

Figure 1. Illustration of the (a) DPS process [29] for the raw spectra (inset) measured from water and ice skin [28]. (b) The minimization of the ""artefacts" of detection" by spectral peak area normalization. The DPS peak area integration features the fraction and the frequency shift features the bond stiffness transition from the ordinary H-O bond vibration mode (valley) to the mode of hydration shell (peak). The raw spectra for aldehydes solvation resolve the significant reflectivity but the DPS minimizes this effect.

The concentration dependent fraction coefficient, $f(C)$, gives direct information on how many bonds being involved in the closest hydration shells. The commonly-shared peak area in Figure 1a is a mixture of the high-order hydration shells and ordinary water, which is out of immediate concern in discussing the nature of hydration. The slope $df_x(C)/dC$ is proportional to the number of hydrating bonds per solute, which varies with the local electric field or the solute-solvent molecular interactions. The solute-solute interactions and H_2O dipole screening will affect the solute electric field and its capability of bond transition.

2.3. Molecular geometric configuration

One needs to clarify the molecular solute structure of aldehydes and formic acids. Solvation dissolves a molecular crystallite into individual molecular solutes. Because of the sp^3-orbital hybridization for C and O atoms upon reaction [25], C=O double bond is unlikely and each O has two pairs of ":".

Therefore, the molecular solute is covered with different numbers of the dangling H^+ and electronic lone pairs ":". The unequal number of the H^+ and the ":" and their asymmetrical distribution surrounding the molecular solute discriminate these molecules one from another with much different properties. Only one oxygen ion short of the aldehyde and different geometry make the aldehyde group completely different from the organic acids.

To meet the criteria of sp^3-orbital hybridization, pairing up the aldehyde molecules is necessary for the formulation such as $2[CH_2O]$ instead of CH_2O. This formulation gives rise to the geometrical mirror symmetry. What differs the acids from the aldehyde is the single or the pairing CH_2 chains. Both the H↔H and the O:⇔:O form in the organic acidic solutions and only the H↔H forms in the aldehydes upon solvation in addition to the O:H-O bonds between solute-solvent O^{2-} anions for all samples. The O-O covalent pairing is necessary to ensure that each O has two bonds and two ":" to realize its sp^3-orbital hybridization [30-32].

Table 2 counts the possible numbers of the O:H-O bonds, the H↔H anti-HBs and the O:⇔:O super-HBs formed between the organic molecules in their aqueous solutions. If there is n(:) number of lone pairs and $p(H^+)$ number protons, the molecular solute will form $n(:) + p(H^+)$ nonbonds between the solute and its neighboring H_2O molecules. Each of the solute H^+ and the ":" has half probability to connect with its alike or unlike of the H_2O molecules. Therefore, among these nonbonds, there will be $|p-n|/2$ number of H↔H (p >n) or O:⇔:O (p<n) and the rest are the O:H vdW bonds. The intermolecular nonbond interactions include O:H, H↔H, O:⇔:O, and electronic polarization without charge sharing or orbital overlapping as the covalent, metallic and ionic bonds.

Table 2. Formulae, geometric configuration and the intermolecular interactions for the formic acids and aldehydes. C and O atoms are subject to sp^3-orbital hybridization with oxygen production of electron lone pairs (paired yellow dots on oxygen in red). The H^+ and ":" surround the molecular solute. The grey spheres represent for C and the blue ones for H^+.

solute	aormic acid			aldehyde		
	methanolic	methanolic	methyl-acetic	form-	acetal-	propion-
formulae	CH_2O_2	$C_2H_4O_2$	$C_3H_6O_2$	$2[CH_2O]$	$2[C_2H_4O]$	$2[C_3H_6O]$

geometry	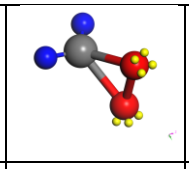	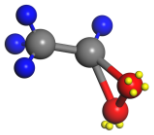	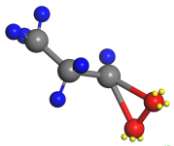			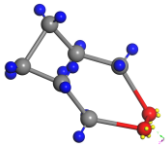
H^+	2	4	6	4	8	12
lone pair (:)	4	4	4	4	4	4
O:H	5	8	9	8	10	12
H↔H	0	0	1	0	2	4
O:⇔:O	1	0	0	0	0	0

The allotropicity of the aldehydes and the organic acids determine the geometry and the polarizability of these molecular dipoles upon solvation. The molecular dipoles and the geometric symmetry could govern the capabilities of these organic molecules and the performance of their solutions. The strong molecular asymmetry determines the solute capabilities of solvent bond and surface stress transforming from the mode of the ordinary water to the hydrating states.

3. Results and discussion

3.1. O:H-O bond Raman spectroscopy

Figure 2 compares the Raman spectra for the organic solutions and ordinary water probed under the ambient conditions. Besides the intramolecular C-H and O-O vibration modes featured at 2900 ± 100 cm^{-1} and 877 cm^{-1}, the spectra show different reflectivity of the solution compared with pure water without significant change of the peak shape. The solute having longer CH_2 chain shows weaker reflectivity at the same concentration, and the reflectivity drops with the increases of the solute concentration. All the spectra show the polarization effect that shifts the O:H frequencies < 300 cm^{-1} to lower frequencies, being the same to solutions of the inorganic salts. The O:H and H-O phonon cooperative relaxation is our main concern and the peak discriminative peak intensities will be minimized by the peak area normalization.

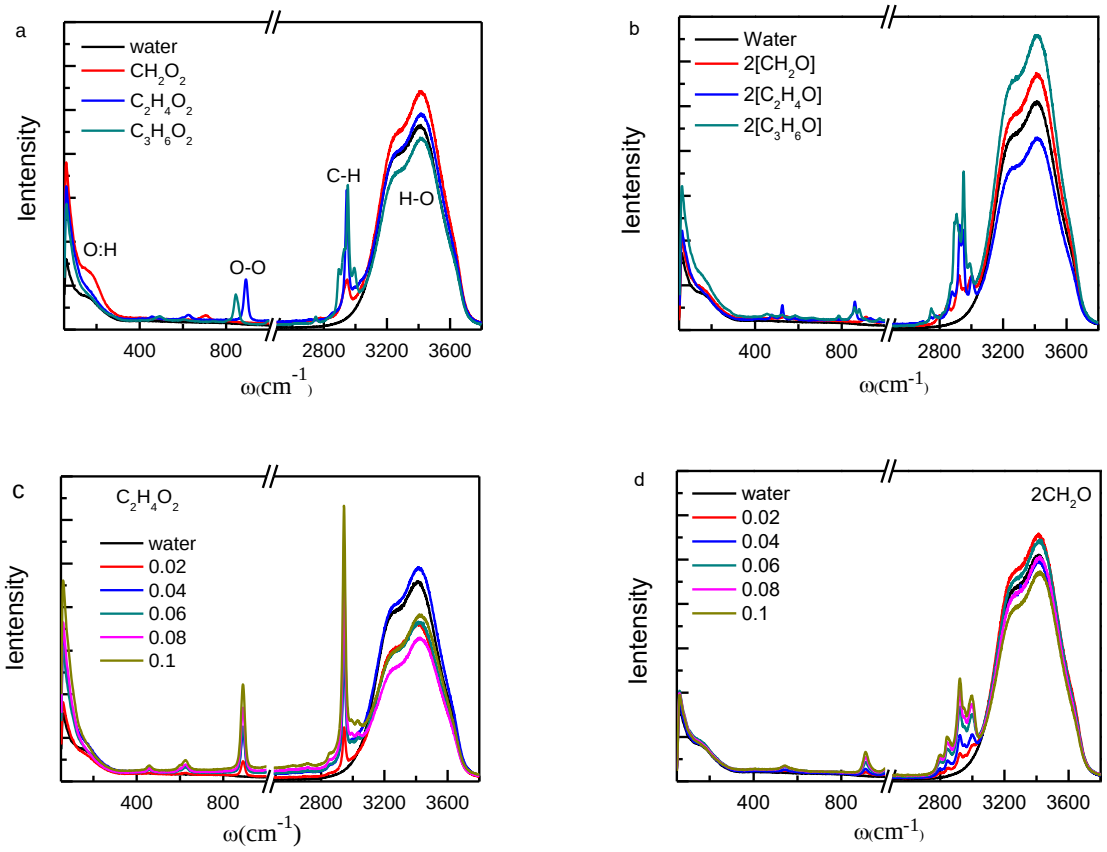

Figure 2. O:H-O bond Raman spectra for (a) the methanoic-, acetic-, and methylacetic-acidic and (b) form-, acet-, propion-aldehyde solutions at 0.04 molar concentration, and the concentration dependence of (c) the acetic acid and (d) formaldehyde solutions with reference to the spectrum of H_2O collected under the same ambient temperature.

3.2. DPS derivatives

The concentration dependence of the ω_x DPS in Figure 3 and Figure 4 shows clearly the polarization effect on the H-O stretching vibration phonon blueshift from 3200 to ~3500 cm^{-1}. The organic acids shift the H-O phonon more above 3500 than to aldehydes centered below 3500 cm^{-1}. The O:H phonon redshifts from 160 to 75 cm^{-1}. The capability of phonon abundance transition of acid is stronger than the aldehydes. The solute electric field will cluster, stretch and polarize the solvent H_2O molecules in the hydration shell. The stretching lengthens and softens the O:H and shortens and stiffens the H-O bond, resulting in the probed phonon frequency shifts [20], as Figure 3a inset showed.

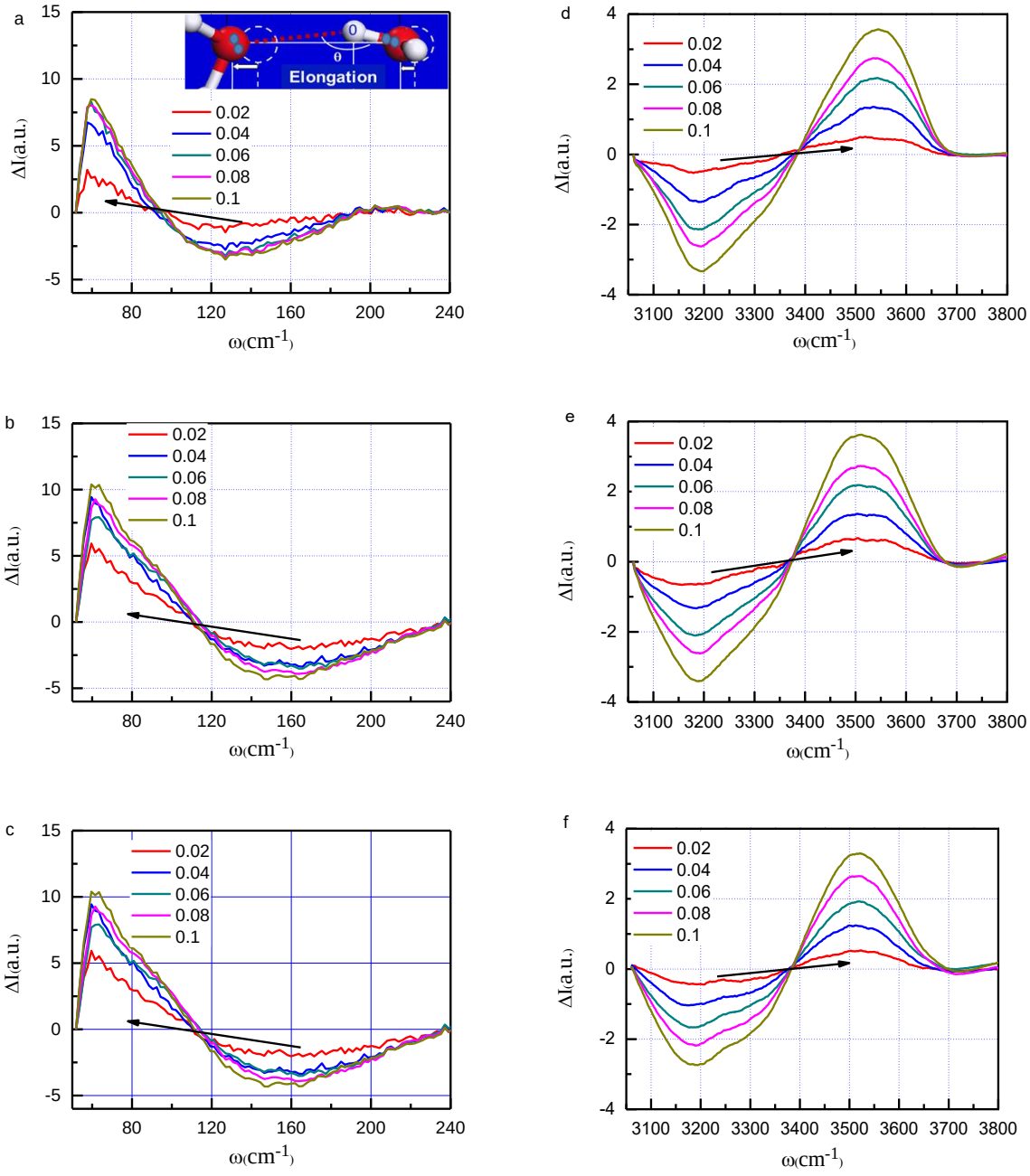

Figure 3. Concentration dependence of the (a-c) ω_L and (d-f) ω_H DPS for (a) methanolic, (b) acetic and (c) methyl-acetic acids under the ambient conditions. Results show consistently the effect of polarization that stiffens the H-O phonon from 3200 to >3500 cm^{-1}, and meanwhile, softens the O:H stretching vibration from 160 to 75 cm^{-1}. Inset a shows the O:H-O bond segmental cooperative relaxation under an electric field [20].

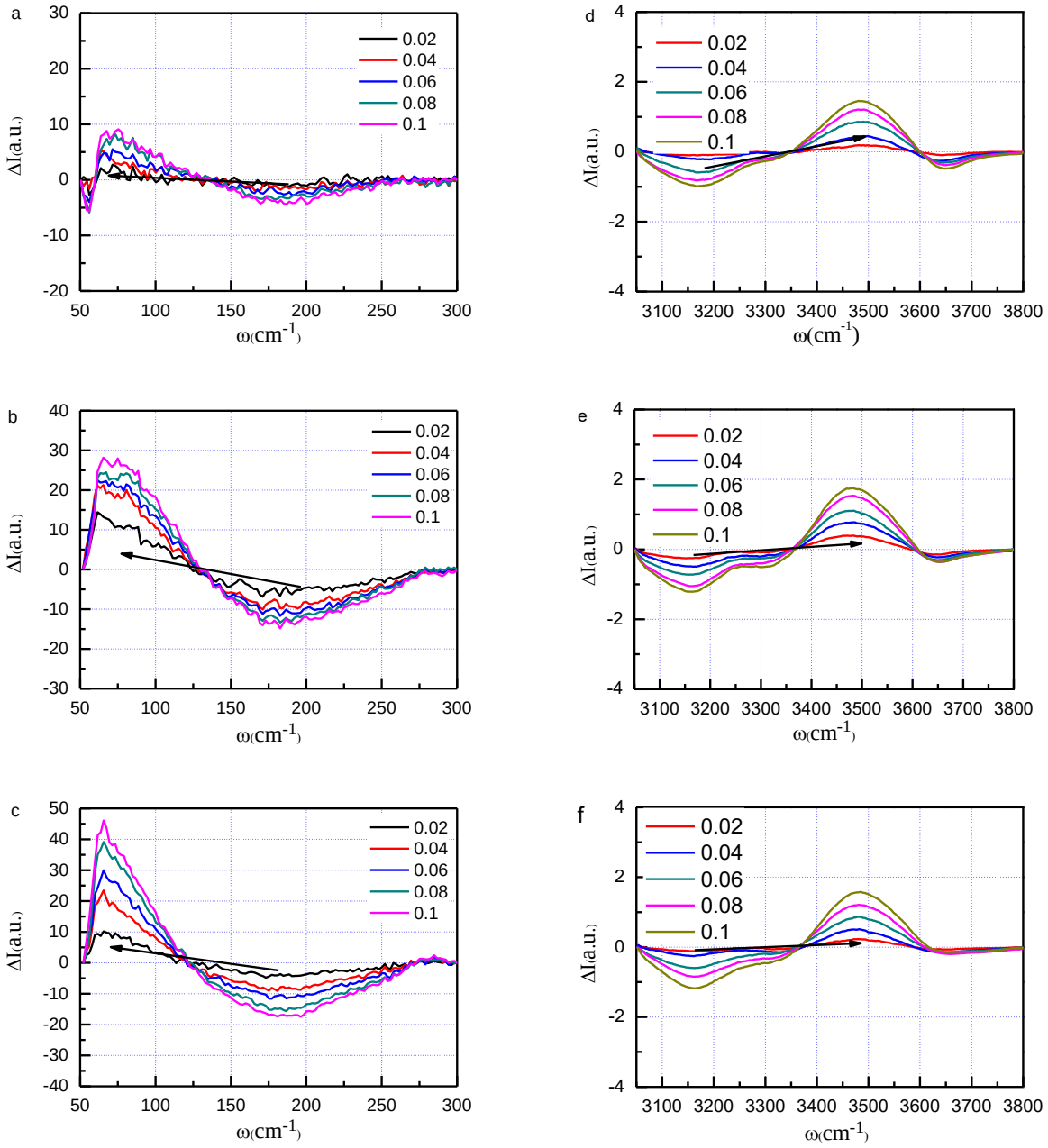

Figure 4. Concentration dependence of the (a-c) ω_L and (d-f) ω_H DPS for the (a, d) formaldehyde, (b, e) acetaldehyde, and (c, f) propionaldehyde showing the strong polarization and relatively weak transition of H-O phonon abundance to the acid solutions.

These molecules form each a giant dipole with the lone pairs ":" gathered at one end and the H^+ protons clustered at the other. The DPS confirms the solute dipole polarization effect on the solvent O:H nonbond and H-O bond, which evidences the presence of the stronger electric field in the hydration shell.

3.2. Fraction Coefficients and contact angles

Figure 5 shows the surface stress and the fraction coefficient as a function of the solute concentration. The contact angles were estimated with a drop sharp analysis system (Krüss GmbH, Germany) by dropping solution droplets onto the copper foil surface at ambient temperature. The value reported was the average of more than 10 measurements made at different positions of the copper foil surface.

The concentration dependence of contact angles between the solutions and the copper foil substrates reveals the manners of solution network and surface stress disruption, which indicates that these molecular solutes have the similar effect of HX acid solvation. Variation of the solution surface stress is related directly to the polarization or depolarization. Ionic polarization [20] and O:⇔:O compression [12] raises the surface stress of salt and basic solution, but thermal fluctuation [33] and H↔H fragilation [11] disrupts the surface stress. However, solvation of the formic acid and aldehyde has the same effect of salt solvation on the O:H-O phonon relaxation but the effect of acid on surface stress disruption. The concentration dependence of the solution surface stress shows that the slope of stress depression is proportional to the CH_2 chain length, or the number of H^+, which is discriminates the manner of stress disruption of the acids and the aldehydes.

The fraction coefficient features the solute capability of bond transition from the mode of ordinary water to the solute hydration shells. The linear dependence of the fraction coefficient for all solutes indicates the invariance of the local electric field and the hydration shell sizes of the solutes because of their dipolar nature. The electric field is anisotropic, locally stronger, and short-range order. The smaller f(C) for aldehydes but stronger surface stress disruption may infer the aldehyde capability of DNA damaging. The linear concentration dependence of the fraction coefficients evidences the invariance of the solute dipolar electric fields.

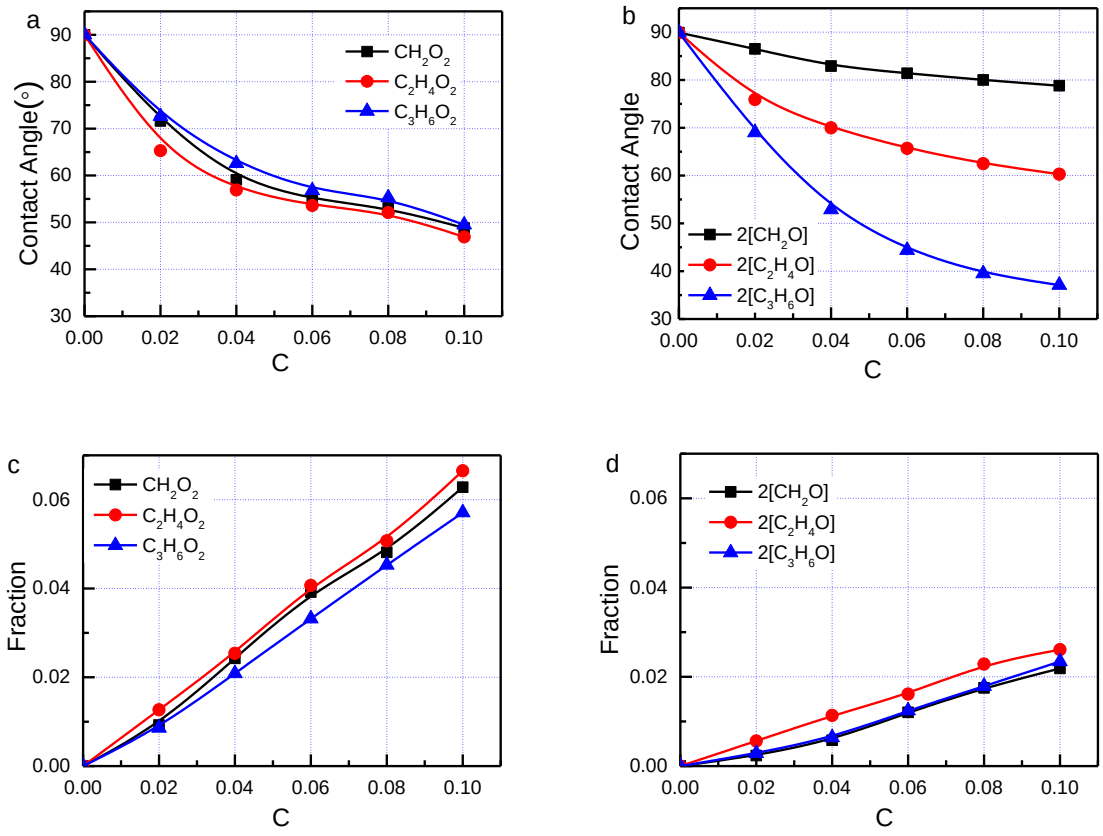

Figure 5. Concentration dependent contact angles for (a) organic acidic and (b) aldehydic solutions and the fraction coefficients for (c) organic acidic and (b) aldehydic solutions. Copper foils serves as the substrate for contact angle detection.

4. Conclusion

The asymmetrical distribution of the H^+ and the ":" makes the molecular solute a dipole with anisotropic, short-range, and strongly localized electric field. The solute dipolar polarization and local structure distortion has the similar effect on the solvent O:H-O bond relaxation and surface stress disruption of protonated acids. The linear concentration trend of the fraction coefficient for bond transition indicates the invariance of the local electric field and the solute hydration shell size. The fact that a smaller fraction of aldehyde disrupts significantly the surface stress may infer its manner of DNA fragmentation, which might be of reference in understanding the cancer factor induced by aldehyde absorption.

Acknowledgement

Financial support received from the Science Challenge Project (No. TZ2016001) and Natural Science Foundation (No. 11502223) of China, Zhejiang Province (No. LY18E060005), Hunan Province (No. 2016JJ3119), and Shen Zhen (No. 827000131).

[1] K. Dong, X. Rao, X. Yang, J. Lin, P. Zhang, Optical Spectroscopy and Spectroscopic Analysis (Chinese), 31 (2011) 3277-3280.
[2] X. Xi, S. Dai, Y. Sun, Envronment Scoience (Chinese), 22 (2001) 19-22.
[3] Z. Xi, F. Tao, D. Yang, Y. Sun, G. Li, H. Zhang, W. Zhang, Y. Yang, H. Liu, Jiournal of Environmental Science (Chinese), 24 (2004) 719-722.
[4] R. Li, Z. Lu, Y. Qiao, H. Yao, F. Yu, X. Yang, Bulletin of Experimental Biology (in Chinese), 37 (2004) 262-268.
[5] Y.N. Jo, I.C. Um, International Journal of Biological Macromolecules, 78 (2015) 287.
[6] F. Greif, O. Kaplan, Critical Care Medicine, 14 (1986) 990-991.
[7] K. Yoshitomi, Y. Matayoshi, H. Tamura, S. Shibasaki, M. Uchida, Y. Haranishi, K. Nakamura, H. Oka, Journal of the Japanese Society of Intensive Care Medicine, 11 (2009) 217-221.
[8] G.M. Tong, S.K. Mak, P.N. Wong, L.O. Kin-Yee, S.O. Sheung-On, C.L. Watt, A.K. Wong, Hong Kong Journal of Nephrology, 2 (2000) 110-112.
[9] S. Kumar, B.V. Babu, (2011).
[10] S. Suwannakham, S.T. Yang, Biotechnology & Bioengineering, 91 (2005) 325.
[11] X. Zhang, Y. Zhou, Y. Gong, Y. Huang, C. Sun, Chem. Phys. Lett., 678 (2017) 233-240.
[12] Y. Zhou, D. Wu, Y. Gong, Z. Ma, Y. Huang, X. Zhang, C.Q. Sun, J. Mol. Liq., 223 (2016) 1277-1283.
[13] Q. Zeng, T. Yan, K. Wang, Y. Gong, Y. Zhou, Y. Huang, C.Q. Sun, B. Zou, PCCP, 18 (2016) 14046-14054.
[14] J. Guo, X. Meng, J. Chen, J. Peng, J. Sheng, X.-Z. Li, L. Xu, J.-R. Shi, E. Wang, Y. Jiang, Nat Mater, 13 (2014) 184-189.
[15] C.Q. Sun, Y. Sun, The Attribute of Water: Single Notion, Multiple Myths, Springer-Verlag, Heidelberg, 2016.
[16] Y.L. Huang, X. Zhang, Z.S. Ma, Y.C. Zhou, W.T. Zheng, J. Zhou, C.Q. Sun, Coord. Chem. Rev., 285 (2015) 109-165.
[17] C.Q. Sun, X. Zhang, X. Fu, W. Zheng, J.-l. Kuo, Y. Zhou, Z. Shen, J. Zhou, J. Phys. Chem. Lett., 4 (2013) 3238-3244.
[18] C.Q. Sun, X. Zhang, J. Zhou, Y. Huang, Y. Zhou, W. Zheng, J. Phys. Chem. Lett., 4 (2013) 2565-2570.
[19] X. Zhang, Y. Xu, Y. Zhou, Y. Gong, Y. Huang, C.Q. Sun, Appl. Surf. Sci., 422 (2017) 475-481.
[20] Y. Zhou, Y. Huang, Z. Ma, Y. Gong, X. Zhang, Y. Sun, C.Q. Sun, J. Mol. Liq., 221 (2016) 788-797.
[21] Y. Gong, Y. Zhou, H. Wu, D. Wu, Y. Huang, C.Q. Sun, Journal of Raman Spectroscopy, 47 (2016) 1351–1359.
[22] Y. Gong, Y. Xu, Y. Zhou, C. Li, X. Liu, L. Niu, Y. Huang, X. Zhang, C.Q. Sun, Journal of Raman Spectroscopy, 48 (2017) 393-398.
[23] Y. Huang, X. Zhang, Z. Ma, Y. Zhou, W. Zheng, J. Zhou, C.Q. Sun, Coordination Chemistry Reviews, 285 (2015) 109-165.
[24] C.Q. Sun, in, United States, 2017.
[25] X.J. Liu, M.L. Bo, X. Zhang, L.T. Li, Y.G. Nie, H. TIan, Y. Sun, S. Xu, Y. Wang, W. Zheng, C.Q. Sun, Chemical Reviews, 115 (2015) 6746-6810.

[26] Y. Zhou, Yuan Zhong, X. Liu, Y. Huang, X. Zhang, C.Q. Sun, J. Mol. Liq., (2017).
[27] X. Wu, W. Lu, W. Ou, M.C. Caumon, J. Dubessy, Journal of Raman Spectroscopy, (2016).
[28] T.F. Kahan, J.P. Reid, D.J. Donaldson, J. Phys. Chem. A, 111 (2007) 11006-11012.
[29] X. Zhang, Y. Huang, Z. Ma, Y. Zhou, W. Zheng, J. Zhou, C.Q. Sun, PCCP, 16 (2014) 22987-22994.
[30] C.Q. Sun, Relaxation of the Chemical Bond, Springer-Verlag, Heidelberg, 2014.
[31] C.Q. Sun, Prog. Mater Sci., 48 (2003) 521-685.
[32] W.T. Zheng, C.Q. Sun, Prog. Solid State Chem., 34 (2006) 1-20.
[33] X. Zhang, T. Yan, Y. Huang, Z. Ma, X. Liu, B. Zou, C.Q. Sun, PCCP, 16 (2014) 24666-24671.